Fabrication of a hybrid PDMS/SU-8/quartz microfluidic chip for enhancing UV absorption whole-channel imaging detection sensitivity and application for isoelectric focusing of proteins

Junjie Ou,[ab] Tomasz Glawdel,[b] Carolyn L. Ren*[b] and Janusz Pawliszyn*[a]

Received 2nd December 2008, Accepted 5th March 2009
First published as an Advance Article on the web 26th March 2009
DOI: 10.1039/b821438g

A poly(dimethylsiloxane)(PDMS)/SU-8/quartz hybrid chip was developed and applied in the isoelectric focusing (IEF) of proteins with ultraviolet (UV) absorbance-based whole-channel imaging detection (UV-WCID). Each hybrid chip was made of three layers: a PDMS flat top substrate, a bottom quartz substrate and a middle layer of SU-8 photoresist. The SU-8 serves two purposes: it contains the microchannel used for IEF separation, and acts as an optical slit that absorbs UV light below 300 nm improving detection sensitivity in WCID. The novel hybrid design demonstrates a two to three times improvement in sensitivity over a comparable PDMS/PDMS design. In addition, the hybrid chip exhibits increased heat dissipation due to the superior thermal conductivity of the bottom quartz substrate allowing for larger electric fields to be used in separations. The hybrid design with IEF-UV-WCID was successful in resolving a complicated sample, hemoglobin control, with high fidelity.

Introduction

Capillary isoelectric focusing (CIEF) is a high-resolution capillary electrophoresis (CE) technique for separating proteins and other zwitterionic compounds that have subtle differences in their structures. CIEF relies on the formation of a stable pH gradient along the length of the capillary so that proteins can be separated according to their different pIs. Several methods exist to set up an axial pH gradient;[1–4] the most popular one uses carrier ampholytes that are mixed with the sample and filled into the capillary. When a high electric field is applied across the capillary, the samples migrate and focus into discrete zones at locations where the local pH is equal to the sample pI. These bands are sharply defined resulting in a high separation resolution and a 50 to 100-fold concentration of the analytes.[5]

Single point detection is often used to identify the bands, which requires transporting the sample by either pressure or electrophoretic means past the detector.[6] However, this process is time consuming and mobilizing the samples results in lower separation efficiency due to dispersion of the bands. An alternative detection method is UV absorbance-based whole-column imaging detection (WCID) developed by Pawliszyn *et al.*,[7–13] which has been successfully employed by Convergent Bioscience Inc. to develop a commercial capillary-based IEF instrument (iCE280 analyzer). In this technique the entire channel is imaged in real-time eliminating the mobilization step, which provides significant gains in both resolution and throughput, as well details of the entire separation process can be revealed. However, the capillary format has inherent limitations as it does not easily integrate with other separation schemes and restricts scale up and, as a consequence, throughput.

Microfluidic chips provide a viable alternative to the capillary format as they offer a number of advantages including low cost, high speed, high throughput, potential for integration, flexibility and portability for a wide range of applications in analytical and bioanalytical chemistry.[14,15] Laser-induced fluorescence (LIF) detection is commonly used in CE microfluidic chips, since higher sensitivity is required with smaller sample volumes[16,17] and many fluorescent reagents for derivatization of analytes are commercially available. However, applying LIF detection techniques also has some disadvantages; the derivatization process is time-consuming and expensive and more importantly it also slightly alters the pI of the analytes.[18–23] Furthermore, fluorescent detectors require a more complex alignment of lenses and filters for accurate detection of the separation channel in comparison to UV absorbance-based detection.

To successfully apply UV absorbance-based detection with microfluidic chips, several issues need to be addressed to improve detection sensitivity and separation performance. For a given imaging detection system such as that used in the iCE280 analyzer, the choice of substrate materials and UV blocking materials is critical. To maximize the detection of the protein samples, all substrates through which UV light passes should be transparent in the UV range (*i.e.* <300 nm). Of the various materials that are available for fabrication, quartz is an ideal option due to its minimal UV absorption. Quartz-based microfluidic chips have a well defined surface chemistry and generally have superior separation performance; however, they are costly and difficult to fabricate using photolithography techniques. As a result, several types of hybrid chips have been developed for UV absorbance-based detection, including glass/fused silica, PVC/silica and PDMS/quartz. For example, Ma *et al.*[24] fabricated a PDMS-quartz chip with a 100 μm thick PDMS

[a]*Department of Chemistry, University of Waterloo, Waterloo, Ontario, Canada N2L 3G1. E-mail: janusz@uwaterloo.ca; Fax: +1 519-746-0435; Tel: +1 519-888-4641*
[b]*Department of Mechanical and Mechatronics Engineering, University of Waterloo, Waterloo, Ontario, Canada N2L 3G1. E-mail: c3ren@mecheng1.uwaterloo.ca; Fax: +1 519-885-5862; Tel: +1 519-888-4567, x 33030*

membrane on the concave detection window for UV absorbance detection, which increased detection sensitivity and extended the detection range by enhancing UV transmittance. In this study as well, a hybrid chip structure of quartz and PDMS was chosen to take advantage of the high transmittance of both materials and the ease of fabricating with conventional soft lithography techniques.

To improve the UV absorbance-based detection sensitivity, optical slits are normally used outside the separation channel region to block stray light from entering the detector. The use of UV blocking slits can be explained as follows. UV absorbance-based detection is based on the Beer–Lambert law:

$$A = \log\left(\frac{I_0}{I}\right) \quad (1)$$

where A is the absorbance of the sample, I_0 is the initial light intensity passing through the channel and I is the light intensity when a sample is present in the channel. The absorbance, A, is directly proportional to the concentration of the sample as long as the law is obeyed. In reality, linearity is limited by chemical and instrumental factors, such as stray light. When stray light is present it leads to:

$$A' = \log\left(\frac{I_0 + I_{\text{stray}}}{I + I_{\text{stray}}}\right) \quad (2)$$

where A' is the absorbance obtained by the instrument and I_{stray} is the stray light intensity from outside of the channel. The existence of stray light limits the dynamic range and reduces the sensitivity of UV detection. For example, when I_{stray} is comparable to I_0, it will read an absorbance of 0.297 for a real absorbance of 2.000, and 0.0028 for a real absorbance of 0.00436. Therefore, blocking stray light from reaching the detector is essential for increasing detection sensitivity and dynamic range of whole-channel UV imaging detection (WCID).

There have been a few methods for integrating an optical slit into a separation chip. For example, Mao *et al.*[25] glued a 50 μm wide metal slit onto a microchannel to ensure UV light only passes through the channel region for enhancing UV absorbance detection. The iCE280 analyzer utilizes a similar approach by gluing a 65 μm wide metal slit to the top substrate of the cartridge used in this instrument. For this method to work properly the slit must be perfectly aligned with the capillary beneath which is a very difficult task even with the aid of a microscope and leads to low success rates. Nakanishi *et al.*[26] fabricated a quartz microchip with a built-in silicon optical slit that improved UV detection sensitivity and avoided misalignment as well. However, the chip was fabricated using conventional photolithography techniques that are very expensive. This study aims to exploit soft lithography techniques that allow optical slits to be built directly into the hybrid quartz-PDMS chip, which can then be evaluated using UV absorbance-based WCID technologies through the iCE280 analyzer.

To our knowledge, there are few studies that incorporate IEF in microfluidic chips using WCID. Fluorescence based WCID using a glass/poly(dimethylsiloxane) (PDMS) microchip for IEF of *R*-phycoerythrin was developed.[27] In this case, an organic light emitting diode was used as the light source. A UV-based WCID detection scheme was also used by Mao *et al.*[25] with a quartz chip and metal slit. More recently, we reported on the development of a poly(dimethylsiloxane) (PDMS)-based microfluidic chip prepared according to rapid prototyping and replica molding techniques for WCID.[28,29] In those designs, a 65 μm wide metal slit similar to that reported by Mao *et al.*[25] was also used. In addition to the tedious work associated with gluing a metal slit on the chip, there was also the problem of non-uniform PDMS thickness which results in optical scattering and distortion of UV light. Solving these limitations motivated the development of a novel design that simplified fabrication procedures while still offering improved detection sensitivity.

Herein a new design is reported where the metal slit is replaced by a built-in SU-8 layer that contains the microchannel and also acts as the optical slit. SU-8 is widely used in microfluidics as either a structural material for channels, a molding material for PDMS replication, or as waveguide in integrated optics.[30,31] In this hybrid chip, the top and bottom of the channel are PDMS and quartz respectively and the sidewalls of the channel are comprised of SU-8, which absorbs UV light at 280 nm and increases the sensitivity of UV-WCID. Utilizing SU-8 as both the channel and optical slit for single point UV detection has been previously reported by Jensen *et al.*[32,33] However, it has not been widely applied for UV absorbance-based detection, and particularly not for WCID. The new hybrid design dramatically simplifies fabrication and shows improved detection sensitivity compared with the previously published PDMS/metal slit design.

Experimental

Materials and reagents

Several types of SU-8 photoresist (SU-8 2005, 2015, 2025 and 2075) and propylene-glycol-monoether-acetate (PGMEA) developer were obtained from Microchem (Newton, MA, USA). Sylgard 184 PDMS prepolymer base and curing agent were purchased from Dow Corning (Midland, MI, USA). Low molecular mass pI markers 4.65, 5.12, 6.14, 7.05, 8.18 were purchased from Bio-Rad (Mississauga, ON, Canada). Myoglobin, carrier ampholytes (CAs) (Pharmalytes 3–10) and methylcellulose (MC) were obtained from Sigma (St. Louis, MO, USA). Poly(vinyl alcohol) (PVA) (MW 13 000–23 000) and polyvinylpyrrolidone (PVP) (MW 360 000) were purchased from Aldrich (Milwaukee, MI, USA). Human hemoglobin control containing HbA, HbF, HbS and HbC was purchased from Helena (Beaumont, TX, USA). Other chemicals were of analytical-reagent grade. Water was purified with an ultrapure system (Barnstead, IA, USA). Quartz slides (3 inch × 1 inch) were purchased from SPI Supplies (West Chester, PA, USA). Nickel metal slit sheets (3 mm × 6.5 cm; slit size, 65 μm × 5 cm) are a custom ordered product from StenTech (Mississauga, ON, Canada).

Fabrication of hybrid microfluidic chip

The fabrication procedure of a hybrid microfluidic chip is shown in Fig. 1A. The quartz substrate was prepared by cleaning in a solution of H_2SO_4/H_2O_2 (3/1, v/v) and then dehydrating on a hot plate at 200 °C for 30 min. A series of negative photomasks with a 5 cm long channel design were commercially printed onto a Mylar film (CAD/Art Services). The thickness of the SU-8 layer

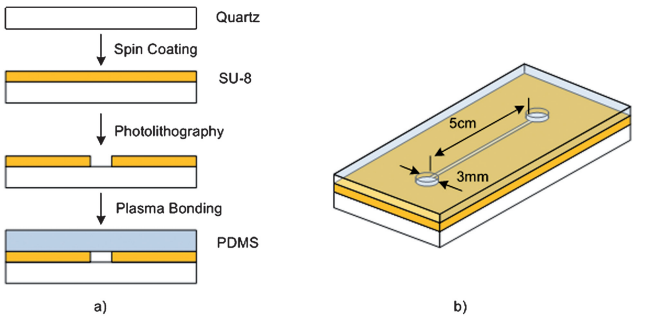

Fig. 1 (A) Diagram of the fabrication process and (B) side view of hybrid PDMS/SU-8/quartz chip.

on the quartz slide varied between 50 μm and 200 μm depending on the spinning speed and viscosity of the SU-8 as recommended by the manufacturer.

A 50 μm thick SU-8 (SU-8 2025) layer was spun onto a quartz substrate with a spin speed of 500 rpm for 25 s followed by a spin-coating speed of 1500 rpm for 30 s. The substrate was subsequently soft baked on a hot plate at 65 °C for 5 min and at 95 °C for 7 min to remove the photoresist solvent. After the substrate cooled to room temperature, UV exposure was performed in a UV mask aligner with a 300 mJ cm^{-2} dose at a wavelength of 365 nm. Post-exposure bake was performed on a hot plate at 65 °C for 5 min and at 95 °C for 6 min successively. After cooling slowly to room temperature, the photoresist was developed in the PGMEA developer for 7 min to dissolve the unexposed SU-8.

PDMS prepolymer was thoroughly mixed with curing agent at a weight ratio of 10 : 1 and degassed for 30 min under vacuum. The mixture was poured onto a blank silicon wafer and cured for 1 h at 80 °C. After curing, the PDMS layer with a thickness of 2 mm was peeled off from the silicon wafer and cut into 1 inch wide pieces. Then, two holes with a 3 mm diameter were punched through the PDMS layer at the reservoir locations. After treatment with oxygen plasma in a Harrick Plasma Cleaner (Harrick Scientific, Ithaca, NY, USA) with a power of 29.6 W for 60 s, both the PDMS layer and quartz substrate were brought into contact and bonded together to enclose the microfluidic channel and complete the chip, as shown in Fig. 1B.

Similarly, other hybrid chips with straight channels of 100 μm wide, 100 μm deep, 5 cm long and 50 μm wide, 200 μm deep, 5 cm long, respectively, were fabricated according to the procedures mentioned above with adjustments made as per the manufactures directions.

Fabrication of PDMS/PDMS microfluidic chip

A PDMS/PDMS microfluidic chip was fabricated using soft lithography and rapid prototyping techniques as detailed in our previous report.[34] Briefly, a PDMS mold containing a 5 cm long straight channel was fabricated from a SU-8 master. The bottom PDMS layer (2 mm thick) was also molded on a blank SU-8 master and two fluidic access holes (3 mm in diameter) were punched at the reservoir locations. After pretreatment using oxygen plasma, these two PDMS layers were brought into contact and bonded together to enclose the microfluidic channel. Because PDMS is flexible, a holder (Convergent Bioscience, Toronto, Canada) with a 1 mm wide, 6 cm long slit was used to support the PDMS chip in order to prevent deformation. In some cases a metal sheet with a 65 μm wide slit was carefully aligned onto the prepared microfluidic chip under an optical microscope so that the slit was exactly positioned and glued over the top of the channel. These PDMS microfluidic chips were patterned with a 5 cm long straight channel with different cross-sectional areas of 100 μm × 100 μm, 50 μm × 50 μm and 50 μm × 200 μm, respectively.

Measurement of chip-based cartridge for isoelectric focusing

The resulting chips were placed in the chamber of the iCE280 analyzer (Convergent Bioscience, Toronto, Canada), which consists of a whole column optical absorption imaging with a deuterium (D2) lamp as the light source. The light beam from the lamp is focused onto the separation channel by a bundle of optical fibers and a cylindrical lens. The UV absorbance image of the whole channel is captured by a CCD camera.

The samples for IEF were prepared in deionized water containing 1.5% PVP, 2% Pharmates (3–10) and pI markers or proteins. The 0.1 mol L^{-1} phosphoric acid and 0.1 mol L^{-1} sodium hydroxide containing 1.5% PVP were used as anolyte and catholyte, respectively. All of the solutions were filtered using a 0.2 μm pore size cellulose acetate filter (Sartorius, Gottingen, Germany) prior to use. After the channel was preconditioned by drawing the PVP solution (1.5%, w/v) with a simple vacuum device for 30 min, the sample was injected with the vacuum device too. Anolyte and catholyte solutions (20 μL for each) were simultaneously added into the left reservoir and right reservoir of the microfluidic chip using two micropipettes. Between runs the channel was washed with the PVP solution for 5 min. Each IEF experiment for a single sample was repeated three times under the same experimental conditions.

Results and discussion

Design of hybrid microfluidic chip for UV-WCID

Fig. 2 illustrates the optical light path for UV absorbance-based detection on three types of microfluidic chips: PDMS/PDMS without a metal slit, PDMS/PMDS with a metal slit, and the hybrid PDMS/SU-8/quartz design. As shown in Fig. 2A, the width of the collimated light beam that illuminates the channel is broader than the width of the microchannel so that both incident light and stray light pass through the bulk material around the channel. In the PDMS/PDMS chip with a metal slit, the slit is narrower than the collimated light beam blocking the light passing through the bulk material from being detected (Fig. 2B), as a result the detection sensitivity is enhanced.[26] In these designs, the slit is 65 μm wide and does not match the channel size, which is either 50 μm wide or 100 μm wide. In the former case stray light can still pass through and reach the detector, leading to a decrease in detection sensitivity, while in the later design the light detected is lower because some of the channel is blocked. In the hybrid design the SU-8 slit serves the same role as the metal slit by absorbing the UV light while also acting as the microchannel side walls (Fig. 2C). An added benefit is that the width of the optical slit is always perfectly matched with the channel width so that the entire sample is illuminated.

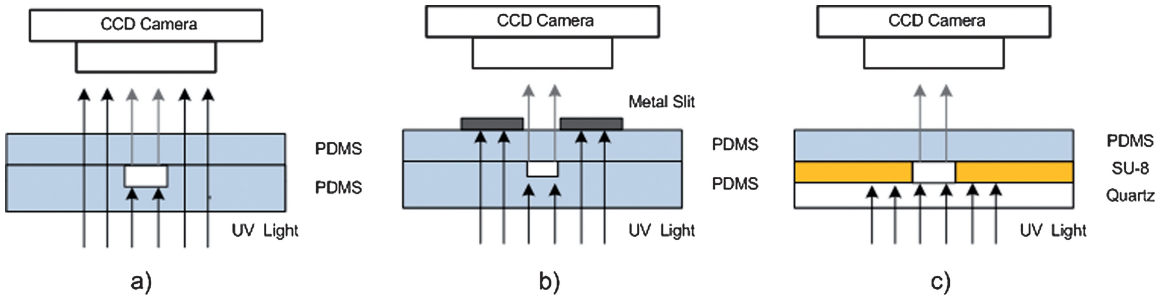

Fig. 2 Schematic light path (side view) for UV absorbance-based detection on (A) PDMS/PDMS microfluidic chip without a metal slit, (B) PDMS/PDMS microfluidic chip with a metal slit, and (C) hybrid chip.

SU-8 contains eight reactive epoxy groups and eight benzene rings in its chemical structure as shown in Fig. 3. The large quantity of epoxy moieties gives SU-8 excellent mechanical and chemical stability against many acids and bases when polymerized. Meanwhile, the benzene ring moieties in the monomer give SU-8 high absorptive property in the UV range (<300 nm). The absorbance of the SU-8 layer is expected to follow the Beer–Lambert law and increases with thickness. To this end, the UV-visible spectrum for polymerized SU-8 layers of thicknesses 50, 100 and 200 μm was characterized by a UV-visible spectrophotometer (Varian, Mississauga, Canada) while a blank quartz slide used as the reference. The absorbance of the 200 μm thick SU-8 layer at 280 nm reached 1.321, which was significantly higher than those of 50 μm and 100 μm thick SU-8, 0.388 and 0.702, respectively. It is evident that SU-8 strongly absorbs UV light and that absorbance dramatically increases with thickness.

To test the performance of the hybrid chip in the iCE280 analyzer, the intensity of the incident light passing through the 100 μm wide, 100 μm deep channel molded in the above-mentioned three different microfluidic chips (PDMS/PDMS with a metal slit, PDMS/PDMS without metal slit and the hybrid PDMS/SU8/quartz) were determined by UV exposure for 300 ms. The PDMS/PDMS chip without a metal slit had the highest detected light intensity (~2000 optical units) followed by the hybrid chip (~1500 optical units) and the PDMS/PDMS chip with a metal slit (~600 optical units). Note that in the PDMS/PDMS chip with a metal slit, the microchannel is also partially blocked since channel width is 100 μm while the slit is 65 μm wide. This results in a significantly lower detected light intensity than the hybrid chip design.

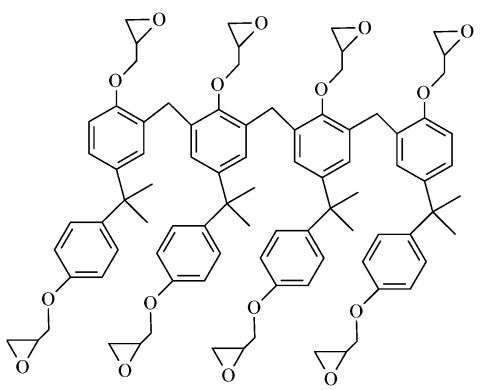

Fig. 3 Molecular structure of SU-8 monomer.

Heat dissipation in hybrid chip design

A great concern in IEF is the temperature gradient that is formed by joule heating because of the high voltages used for separation. An increase in temperature affects various physical properties of the solution which can adversely influence the stability of electroosmotic flow and separation efficiency.[35] Heat dissipation is therefore an important consideration in chip design, particularly for polymer-based chips that are good thermal insulators.

In this case, heat dissipation in the hybrid chip design with various channel dimensions was investigated by measuring the relationship between current and applied voltage to determine an Ohm's law plot as shown in Fig. 4. The current increased linearly with the applied voltage in the range of 100 to 600 V cm^{-1} in both PDMS/PDMS and hybrid PDMS/SU-8/quartz chip designs under the same operating conditions. The linearity indicates that Joule heating is negligible under these conditions.

Comparing the current–voltage relationship of the PDMS/PDMS and hybrid chip designs, one can find that the hybrid chip design has better heat dissipation which is due to the different thermal conductivities of the chip substrates used in these two

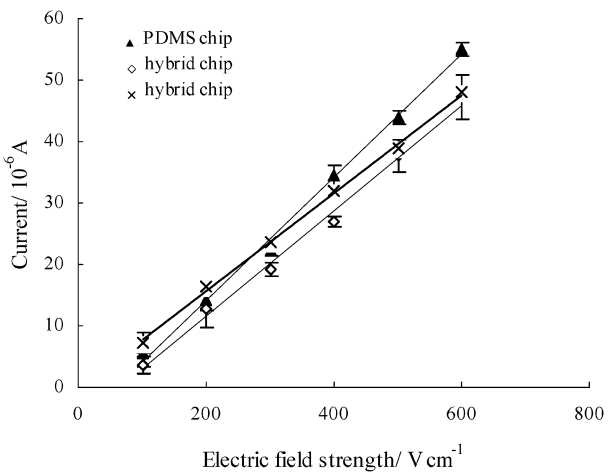

Fig. 4 Heat dissipation in both PDMS patterned the 5 cm long channel of 100 μm wide, 100 μm deep (▲) and hybrid microfluidic chips patterned the channel of 100 μm wide, 100 μm deep, (◇) and 50 μm wide, 200 μm deep (×), respectively, in 5 mM NaCl solution.

designs. In the hybrid chip design, one of the chip substrates is quartz which has a high thermal conductivity of 1.46 W m^{-1} K^{-1},[35] while PDMS and SU8 have a much lower value of around 0.2 W m^{-1} K^{-1}.[35,36] This indicates that a higher voltage difference can be employed in the hybrid chip design to achieve fast protein separation. There is a small variation in the current–voltage relationship for the hybrid chip design with different channel dimensions (100 μm × 100 μm and 50 μm × 200 μm) as shown in Fig. 4. This may be caused by nonuniformity of chip substrates and channel dimensions. Theoretically, the two chips should have the same relationship if other operating conditions are the same because they have the same cross-sectional area (10 000 μm^2) which gives rise to the same heating source and heat dissipation.

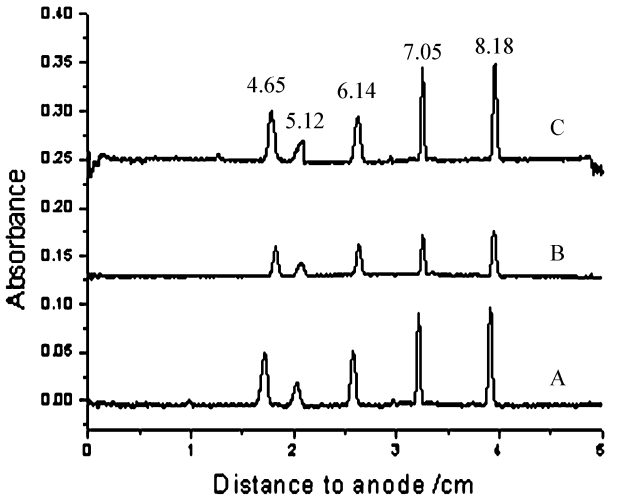

Fig. 5 Separation of five pI markers (4.65, 5.12, 6.14, 7.05, 8.18) on the (A) hybrid chip, (B) PDMS/PDMS microfluidic chip without a metal slit and (C) PDMS microfluidic chip with a metal slit by IEF-WCID, respectively. The samples containing 2% Pharmalytes (pH 3–10) were added PVP (1.5%, w/v). The applied voltage was set at 1500 V for 15 min. The patterned channel is 200 μm in depth, 50 μm in width and 5 cm in length.

Electro-osmotic flow suppression

Electro-osmotic flow (EOF) must be suppressed in order to eliminate sample peaks from drifting when performing IEF-WCID. In the hybrid chip design eliminating EOF is compounded by the fact that the microchannel is composed of three distinct materials, PDMS (top substrate), SU-8 (channel side walls) and quartz (bottom substrate). In native PDMS channels EOF is pH-dependent and PDMS is known to absorb proteins due to its hydrophobic properties.[37] Plasma treatment alters the surface chemistry of PDMS channels and makes PDMS material hydrophilic, however, the treatment is temporary and the resulting EOF is highly unstable. Quartz produces a stable EOF that is significantly higher than that generated on PDMS, while SU-8 typically has a value similar to glass channels at pH levels above 4.[36] Consequently, it is expected that the hybrid chip design will generate EOF if the microchannel surfaces are not chemically treated.

The common method for eliminating EOF and absorption of proteins is to permanently or dynamically coat the channel wall with neutral hydrophilic polymers, such as methylcellulose[38] or hydroxylpropylmethyl cellulose.[39] As well, PVP has been found to be a good additive in the samples for IEF-WCID to suppress EOF in PDMS/PDMS microfluidic chips as reported previously.[28,29] In this case, the effects of different polymers, MC, PVA and PVP, on suppressing EOF in the hybrid chip designs were tested. When MC or PVA was used, the focused zones moved from anode to cathode eventually exiting the channel, suggesting that EOF was only partially suppressed. However, the mobilization of the focused zones was barely observed when a higher concentration of PVP (≥1.5%, w/v) was used as an additive. Furthermore, higher concentrations of PVP increase the fluid viscosity and help suppress mobilization caused by hydrodynamic pressure driven flow between the two reservoirs.

Application of hybrid chip for IEF-UV-WCID

All three chip designs were evaluated by separating pI markers (4.65, 5.12, 6.14, 7.05, 8.18) in the same channel dimension (5 cm long, 200 μm deep, 50 μm wide). The separation results for the hybrid chip design, the design of PDMS/PDMS chip without a metal slit and the design of PDMS/PDMS chip with a metal slit are shown in Fig. 5. All peaks of the pI markers for the hybrid chip design (Fig. 5A) are sharp and symmetric, indicating the successful prevention of EOF and adsorption of analytes by dynamic coating of PVP. A linear pH gradient was obtained by plotting the peak position versus the pI values of the pI markers (data not shown), and the linear correlation coefficient reached 0.9996 ($n = 5$).

The separation results also show that the detection sensitivity of the hybrid design is equivalent to the PDMS/PDMS chip with a metal slit and significantly greater than the no slit design. It can be seen that the separation peak height in the hybrid chip design is two times of that of the PDMS/PDMS chip without a metal slit (Fig. 5A and B). This may be attributed to two reasons. Quartz was used because of its higher transparency for UV light than PDMS, facilitating the enhancement of UV absorbance-based detection. In addition, the SU-8 layer in this hybrid chip composing the channel side walls has the function of the optical slit, which can essentially prevent stray light from reaching the detector minimizing the influence of scattered light. It can be seen from Fig. 5A and 5C that the detection sensitivity of the hybrid design is equivalent to the PDMS/PDMS chip design with a metal slit. For the peak of pI 7.05, the height of the metal slit design is slightly lower than that of the hybrid design. This is due to the metal optical slit (65 μm wide) being wider than the 50 μm wide microchannel which allows for more incident light to reach the CCD camera, leading to a slightly lower sensitivity and absorbance value.

To further validate that the hybrid chip design provides superior performance over the PDMS/PDMS chip design, IEF-WCID was also performed for a horse heart myoglobin sample on both chip designs. In both designs, a 100 μm deep, 100 μm wide microchannel was used. The chips were calibrated first using four pI markers as shown in Fig. 6A. The peak heights obtained on the hybrid chips were 2–3 times greater than those obtained on PDMS/PDMS chips without a metal slit. The separation results of the horse heart sample are shown in Fig. 6B

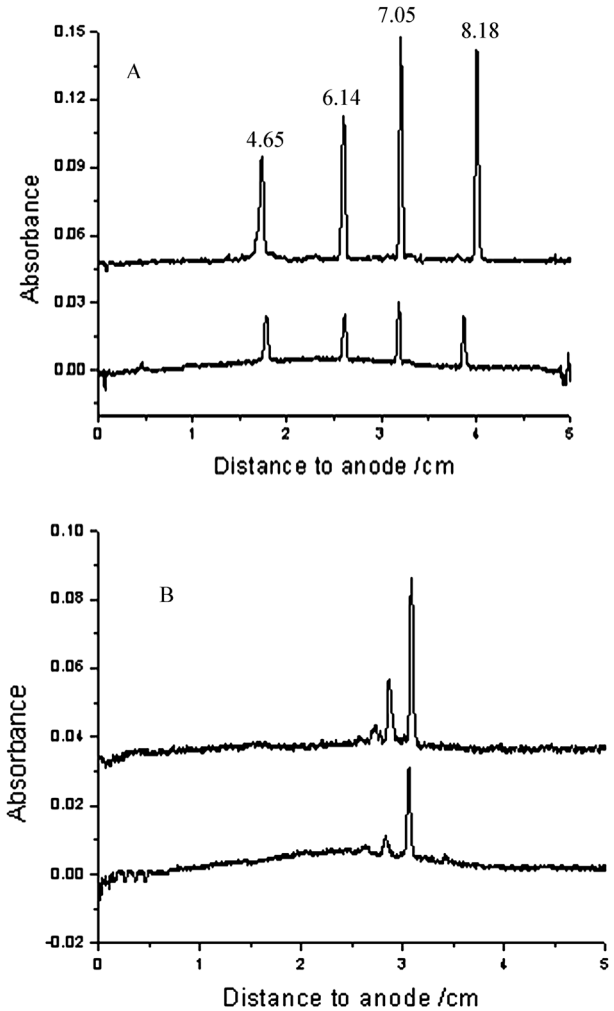

Fig. 6 Separation of (A) four pI markers (4.65, 6.14, 7.05, 8.18) and (B) horse heart myoglobin on the hybrid chip (top) and PDMS/PDMS chip without metal slit (bottom) by IEF-UV-WCID, respectively. The samples containing 2% Pharmalytes (pH 3–10) were added PVP (1.5%, w/v). The applied voltage was set at 1500 V. The patterned channel is 100 μm deep, 100 μm wide and 5 cm long.

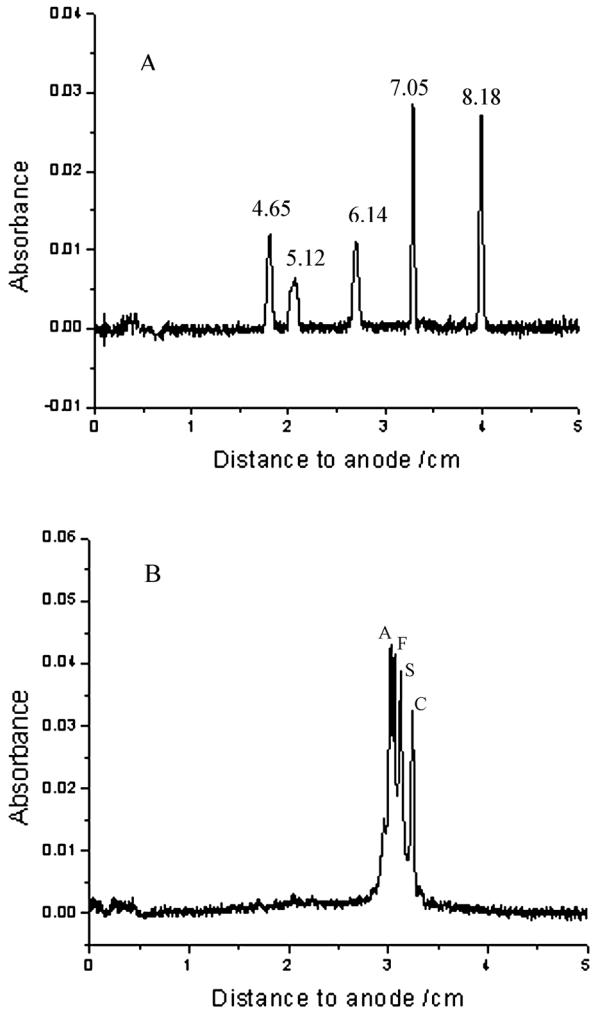

Fig. 7 Separation of (A) five pI markers (4.65, 5.12, 6.14, 7.05, 8.18) and (B) hemoglobin control on the hybrid chip IEF-WCID, respectively. The samples containing 2% Pharmalytes (pH 3–10) were added PVP (1.5%, w/v). The applied voltage was set at 1500 V for 15 min. The patterned channel is 50 μm in depth, 50 μm in width and 5 cm in length.

where two peaks could be clearly observed on both chip designs. These two peaks may be assigned to the two isoforms contained in the myoglobin sample from a horse heart, whose pIs are 6.8 and 7.2, respectively. Additionally, an unknown peak marked by the asterisk could be clearly observed on the hybrid chip design but not on the PDMS/PDMS chip design. This is because of the higher sensitivity of the UV absorbance-based detection on the hybrid chip and demonstrates the advantages of the hybrid chip design. The pI of the unknown ingredient was determined to be 6.55.

The separation of 5 pI markers and hemoglobin control using the IEF-UV-WCID technology was completed on the hybrid chip with a 50 μm deep, 50 μm wide microchannel. Five pI markers were separated perfectly and a horizontal baseline was exhibited as shown in Fig. 7A. A more complicated sample, human hemoglobin control AFSC, containing four definite isoforms (A, 7.0; F, 7.1; S, 7.3; C, 7.5) and whose pI values are very close, was selected as the sample for evaluating the resolving power of the hybrid chip. As shown in Fig. 7B, four isoforms were separated very well. Unlike the previous results with 100 μm and 200 μm thick SU-8, detection sensitivity of 50 μm design did not show an improvement in detection sensitivity in comparison to the two PDMS/PDMS chip designs (data not shown) by analyzing peak heights. The lack of improvement can be attributed to the thinner SU-8 layer which resulted in less absorbance of stray light. Based on these results it can be concluded that the benefits of using an SU-8 optical slit are only prevalent in SU-8 layers thicker than 50 μm.

A run-to-run repeatability test was performed for the hybrid chip design by comparing the calibrated pI and peak height of a given sample for three runs under the same operating conditions. The chip-to-chip reproducibility was also investigated by comparing the calibrated pI and peak height of a given sample separated in three separate hybrid chips. The pI of 7.05 was calibrated and measured to be 7.05 ± 0.01. The peak heights of pI 7.05 for all runs are listed in Table 1. The relative standard deviations (RSD) are less than 1% ($n = 3$) for run-to-run repeatability, and less than 2% ($n = 3$) for chip-to-chip

Table 1 Repeatability and reproducibility of hybrid chips for IEF-WCID of proteins

Parameter	Peak height[a]			Run-to-run RSD	Chip-to-chip RSD
	Run 1	Run 2	Run 3		
Chip 1	0.0891	0.0901	0.0908	0.98%	1.93%
Chip 2	0.0911	0.0925	0.0920	0.84%	
Chip 3	0.0880	0.0884	0.0892	0.81%	

[a] The peak height was the absorbance of pI 7.05 in the pI mixture samples. The IEF conditions are the same as in Fig. 5.

reproducibility. The lifetime of the hybrid chip was also evaluated by performing 50 consecutive separations of hemoglobin control on a single chip. The separation performance was not changed after 50 runs by comparing the resolution of hemoglobin control and their peak heights, which is likely due to the elimination of gluing a metal slit to the chip. These results indicated that reproducibility of the hybrid chip is more than satisfactory.

Conclusions

A PDMS/SU-8/quartz hybrid chip was developed and successfully applied for separating proteins and pI markers using the IEF-UV-WCID technology. This hybrid design exhibits several advantages. First, the fabrication procedure of the hybrid chip was greatly simplified by using soft lithography techniques compared to the commercial cartridge used in the iCE280 analyzer which also utilizes IEF-UV-WCID technology for analysis. Second, the SU-8 layer which acts as both the channel side walls and optical slit can be patterned onto a quartz slide eliminating the costly fabrication required using conventional photolithography technology for silicon-based chips and optical slits. Third, the UV absorbance-based detection sensitivity can be enhanced on the hybrid chip-based cartridge for IEF of proteins and pI markers compared with that on the PDMS/PDMS chips without a metal slit. Final, heat dissipation is improved on the hybrid chips compared to PDMS/PDMS chips due to the higher thermal conductivity of quartz compared to PDMS. The separation performance of the hybrid chip was validated using both pI markers and proteins. The proposed concept can be extended to multi and complex channel structures. The chips containing the light blocking layer can be placed directly on the CCD two dimensional sensor eliminating need for optics.

Acknowledgements

The authors gratefully acknowledge Dr Tiemin Huang of the Convergent Bioscience Ltd, Toronto, Canada, for assistance with the fabrication of chips. This work was supported by the Strategic Project Grant from the Natural Sciences and Engineering Research Council of Canada (NSERC).

References

1 T. M. Huang and J. Pawliszyn, *Electrophoresis*, 2002, **23**, 3504–3510.
2 T. M. Huang, X. Z. Wu and J. Pawliszyn, *Anal. Chem.*, 2000, **72**, 4758–4761.
3 J. Pospichal, J. Chmelik and M. Deml, *J. Microcolumn Sep.*, 1995, **7**, 213–219.
4 J. Budilova, J. Pazourek, P. Krasensky and J. Pospichal, *J. Sep. Sci.*, 2006, **29**, 1613–1621.
5 N. J. Clarke, A. J. Tomlinson, G. Schomburg and S. Naylor, *Anal. Chem.*, 1997, **69**, 2786–2792.
6 C. X. Zhang, F. Xiang, L. Pasa-Tolic, G. A. Anderson, T. D. Veenstra and R. D. Smith, *Anal. Chem.*, 2000, **72**, 1462–1468.
7 J. Q. Wu and J. Pawliszyn, *J. Chromatogr. B*, 1994, **657**, 327–332.
8 J. Q. Wu and J. Pawliszyn, *Electrophoresis*, 1995, **16**, 670–673.
9 Q. L. Mao and J. Pawliszyn, *J. Biochem. Biophy. Methods*, 1999, **39**, 93–110.
10 T. M. Huang and J. Pawliszyn, *Analyst*, 2000, **125**, 1231–1233.
11 Z. Liu and J. Pawliszyn, *Anal. Chem.*, 2003, **75**, 4887–4894.
12 Z. Liu and J. Pawliszyn, *J. Proteome Res.*, 2004, **3**, 567–571.
13 X. Z. Wu, T. M. Huang, Z. Liu and J. Pawliszyn, *Trends Anal. Chem.*, 2005, **24**, 369–382.
14 D. R. Reyes, D. Iossifidis, P. A. Auroux and A. Manz, *Anal. Chem.*, 2002, **74**, 2623–2636.
15 P. A. Auroux, D. Iossifidis, D. R. Reyes and A. Manz, *Anal. Chem.*, 2002, **74**, 2637–2652.
16 S. Gotz and U. Karst, *Anal. Bioanal. Chem*, 2007, **387**, 183–192.
17 X. M. Xu, L. Li and S. G. Weber, *Trends Anal. Chem.*, 2007, **26**, 68–79.
18 P. J. Viskari and J. P. Landers, *Electrophoresis*, 2006, **27**, 1797–1810.
19 M. A. Schwarz and P. C. Hauser, *Lab Chip*, 2001, **1**, 1–6.
20 L. J. Jin, B. C. Giordano and J. P. Landers, *Anal. Chem.*, 2001, **73**, 4994–4999.
21 A. M. Garcia-Campana, M. Taverna and H. Fabre, *Electrophoresis*, 2007, **28**, 208–232.
22 S. Suzuki, N. Shimotsu, S. Honda, A. Arai and H. Nakanishi, *Electrophoresis*, 2001, **22**, 4023–4031.
23 K. W. Ro, K. Lim, B. C. Shim and J. H. Hahn, *Anal. Chem.*, 2005, **77**, 5160–5166.
24 B. Ma, X. Zhou, G. Wang, Z. Dai, J. Qin and B. Lin, *Electrophoresis*, 2007, **28**, 2474–2477.
25 Q. L. Mao and J. Pawliszyn, *Analyst*, 1999, **124**, 637–641.
26 H. Nakanishi, T. Nishimoto, A. Arai, H. Abe, M. Kanai, Y. Fujiyama and T. Yoshida, *Electrophoresis*, 2001, **22**, 230–234.
27 K. N. Ren, Q. L. Liang, B. Yao, G. Luo, L. D. Wang, Y. D. Gao, Y. M. Wang and Y. Qiu, *Lab Chip*, 2007, **7**, 1574–1580.
28 Z. Liu, J. Ou, R. Samy, T. Glawdel, T. Huang, C. L. Ren and J. Pawliszyn, *Lab Chip*, 2008, **8**, 1738–1741.
29 J. Ou, T. Glawdel, R. Samy, S. Wang, Z. Liu, C. L. Ren and J. Pawliszyn, *Anal. Chem.*, 2008, **80**, 7401–7407.
30 T. A. Anhoj, A. M. Jorgensen, D. A. Zauner and J. Hubner, *J. Micromech. Microeng.*, 2006, **16**, 1819–1824.
31 P. Abgrall, V. Conedera, H. Camon, A. M. Gue and N. T. Nguyen, *Electrophoresis*, 2007, **28**, 4539–4551.
32 R. J. Jackman, T. M. Floyd, R. Ghodssi, M. A. Schmidt and K. F. Jensen, *J. Micromech. Microeng.*, 2001, **11**, 263–269.
33 H. Lu, M. A. Schmidt and K. F. Jensen, *Lab Chip*, 2001, **1**, 22–28.
34 D. C. Duffy, J. C. McDonald, O. J. A. Schueller and G. M. Whitesides, *Anal. Chem.*, 1998, **70**, 4974–4984.
35 Y. Zhang, N. Bao, X. Yu, J. Xu and H. Chen, *J. Chromatogr. A*, 2004, **1057**, 247–251.
36 T. Sikanen, S. Tuomikoski, R. A. Ketola, R. Kostiainen, S. Franssila and T. Kotiaho, *Lab Chip*, 2005, **5**, 888–896.
37 Y. Li, D. L. DeVoe and C. S. Lee, *Electrophoresis*, 2003, **24**, 193–199.
38 H. C. Cui, K. Horiuchi, P. Dutta and C. F. Ivory, *Anal. Chem.*, 2005, **77**, 1303–1309.
39 B. Yao, H. H. Yang, Q. L. Liang, G. Luo, L. D. Wang, K. N. Ren, Y. D. Gao, Y. M. Wang and Y. Qiu, *Anal. Chem.*, 2006, **78**, 5845–5850.

